JOURNAL OF APPLIED ELECTROCHEMISTRY 22 (1992) 973–977

High area Ni–Zn and Ni–Co–Zn codeposits as hydrogen electrodes in alkaline solutions

M. J. DE GIZ, S. A. S. MACHADO, L. A. AVACA, E. R. GONZALEZ

Instituto de Física e Química de São Carlos/USP C.P. 369, 13560, São Carlos, SP, Brazil

Received 3 September 1991; accepted 12 January 1992

This paper describes the preparation of Ni–Zn and Ni–Co–Zn coatings by electrodeposition on a mild steel substrate. After treatment in a KOH solution to leach out part of the zinc, the materials were evaluated as cathodes for the hydrogen evolution reaction in alkaline solutions. The materials were found to have high surface areas and low Tafel slopes. Overpotentials at current densities of technological interest are significantly lower than those of the traditional materials used in water electrolysis.

1. Introduction

Of the several ways in which hydrogen can be obtained, water electrolysis has many advantages [1], particularly from the environmental point of view [2], but it has the disadvantage of producing hydrogen at a higher cost [3]. Unpressurized unipolar electrolysers operating with nickel electrodes in 28% KOH at 70° C and a current density of 135 mA cm^{-2} shown an overpotential of about 400 mV for both the hydrogen evolution and oxygen evolution reactions (HER and OER) [4]. Adding the thermodynamic potential for the reaction at this temperature (1.19 V) and the ohmic potential drop (about 0.2 V) the operational voltage of the electrolyzer exceeds 2.2 V.

Various cathode materials have been found to reduce the corresponding overpotential. Conway *et al.* [5, 6] studied a Ni–Mo–Cd codeposit and concluded that the higher activity of this material is associated to both an increase in effective area and changes in the properties of the adsorbed species. Vanderborre *et al.* [7] studied the activation of Ni–S codeposits with cathodic polarization and proposed the existence of a hydrogen layer in the form a hydride which is responsible for the activation of the electrode. A similar study was recently reported by Sabela and Paseka [8] showing a loss of activity after prolonged cathodic polarization. Endoh *et al.* [9] prepared Ni–Raney cathodes by incorporating Ni–Raney powder into a nickel deposition bath. These electrodes had high activity and low Tafel slopes. Brossard *et al.* [10] have studied large area cathode materials, mainly Ni–Raney type coatings obtained from Ni–Al alloys prepared by plasma spraying. Fiori and Mari [11] carried out a general comparative study of several materials like Ni–Mo, Ni–Raney, Ni–S, Ni–Co–S and others. Gonzalez *et al.* [12, 13] studied the HER on Ni–Fe and Fe and concluded that the improvement observed in these materials is due to both an increased effective area and an enhanced catalytic activity. Divisek *et al.* [14] have shown the advantages of preparing Raney type electrodes from the galvanic deposition of a Ni–Zn alloy and studied their performance as well as that of Ni–Mo and Ni–Mo–Cd coatings. Recently, Arul Raj and Vasu [15] examined the HER on several nickel alloys deposited on mild steel and concluded that Ni–Zn has (after leaching out the zinc) a good electrocatalytic effect, although the best material according to these authors was Ni–Mo.

This paper describes a more detailed electrochemical evaluation of Ni–Zn and Ni–Co–Zn codeposits as cathode materials with improved characteristics for the HER. The materials were studied by cyclic voltammetry and steady-state polarization with the aim of distinguishing between high effective area and real catalytic effects and were also tested for long term operation.

2. Experimental details

Codeposits of Ni–Zn and Ni–Co–Zn were obtained on a mild steel substrate with the following main components: 0.102% C, 0.05% Si, 0.62% Mn, 0.09% P, 0.019% S and 0.016% Mg. The mild steel substrates were polished with 600 grit emery paper and washed prior to the introduction in the deposition baths which had the compositions (in g dm^{-3}) shown in Table 1.

The electrodepositions were carried out using a nickel anode in a slowly agitated bath, at 50° C and a current density of 50 mA cm^{-2} applied for 1 h. In both cases the pH was 4.5. These are typical deposition conditions [16] with a proper current density to produce thick and rough deposits. The average thickness of the deposits was about 40 μm. In all cases the chemicals were p.a. quality and used without further purification. After the depositions the electrodes were treated for 10 h in a 28% KOH solution at room temperature.

Electrolyte solutions used in the HER experiments were prepared with recrystallized KOH or NaOH (Merck, p.a.) and pre-electrolysed at room temperature with 5 cm^2 nickel electrodes for 48 h at 5 mA cm^{-2}. After this procedure the iron content, determined by square wave voltammetry, was always below 20 p.p.b. The water used to make these solutions was purified in a Millipore Q system.

0021-891X/92

Table 1. Bath compositions

Composition /g dm^{-3}	*Deposits*	
	Ni–Zn	*Ni–Co–Zn*
$NiSO_4 \cdot 6H_2O$	330	330
$NiCl_2 \cdot 6H_2O$	45	45
$CoSO_4 \cdot 6H_2O$	–	19
H_3BO_3	37	37
$ZnCl_2$	20	20

Electrochemical experiments were conducted with 0.5 cm^2 electrodes in a three-compartment glass cell. The auxiliary electrode was a 2 cm^2 platinum foil separated from the main compartment by a porous glass frit. A Hg/HgO/HO$^-$ reference electrode was joined to the main compartment via a Luggin capillary. EDX analysis of the cathode surface after long term electrolysis showed no sign of Pt contamination from the counter electrode. Electrochemical measurements were carried out using a computer controlled PAR mod. 273 potentiostat with ohmic drop compensation.

Additional experiments were done with 200 cm^2 electrodes under conditions simulating the operation of a unipolar electrolyser. The working electrode was placed in a 4 dm^3 cell between two electrodeposited nickel anodes of the same geometric area. The cathode was inside an extra fine nylon cloth to avoid mixing of the evolved gases.

3. Results and discussion

3.1. *Characterization of the electrodeposits*

The chemical composition of the electrodeposits was determined by square wave voltammetry and atomic absorption spectroscopy after removal and dissolution of the electrodeposited layer in aqua regia. This procedure was applied on samples before and after treatment with KOH in order to establish how much zinc is removed from the electrodeposited material. The results are presented in Table 2 and suggest that the treatment leaves a surface rich in nickel over a Ni–Zn or a Ni–Co–Zn base. The figures for the treated Ni–Zn material are very similar to those reported previously [15].

Figure 1 shows the X-ray diffractograms of treated Ni–Zn and Ni–Co–Zn codeposits (in this case prepared on copper substrates). It shows a combination

Table 2. Composition of the electrodeposits, in at. %, before and after treatment with 28% KOH solution for 10 h at room temperature

Material	*Ni*	*Zn*	*Co*
Ni–Zn			
Untreated	18	82	–
Treated	54	44	–
Ni–Co–Zn			
Untreated	16	78	6
Treated	52	36	12

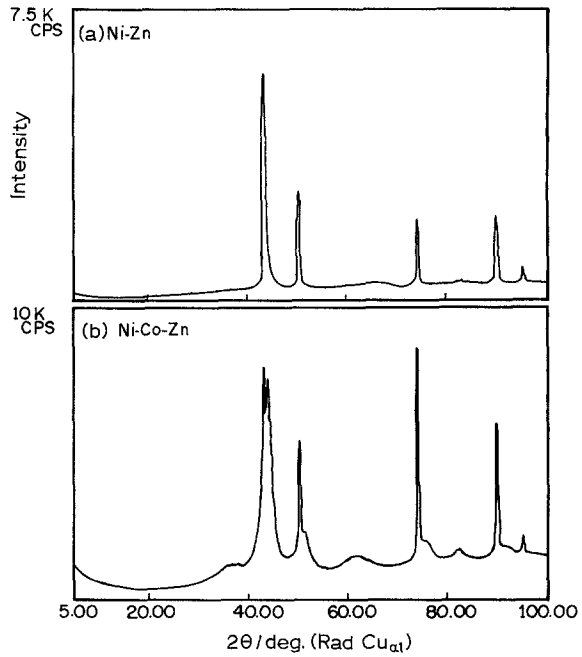

Fig. 1. X-ray diffractograms for (a) Ni–Zn and (b) Ni–Co–Zn as prepared by electodeposition and leaching.

of sharp lines at 2θ = 43.29, 50.43, 74.13, 89.93 and 95.13 due to the copper substrate with associated broad bands from the electrodeposits which are characteristic of either amorphous or microcrystalline materials. Thus, the samples were heated at 400° C for 1 h in an argon atmosphere to promote crystallization. The diffractograms obtained after this treatment are presented in Fig. 2 and show a large number of peaks corresponding to Ni and Zn, and Ni, Co and Zn, respectively. Further investigations are necessary to fully characterize the crystallographic structure of these alloys. Nevertheless, the electrochemical activity of these materials after heat treatment is always lower than before it.

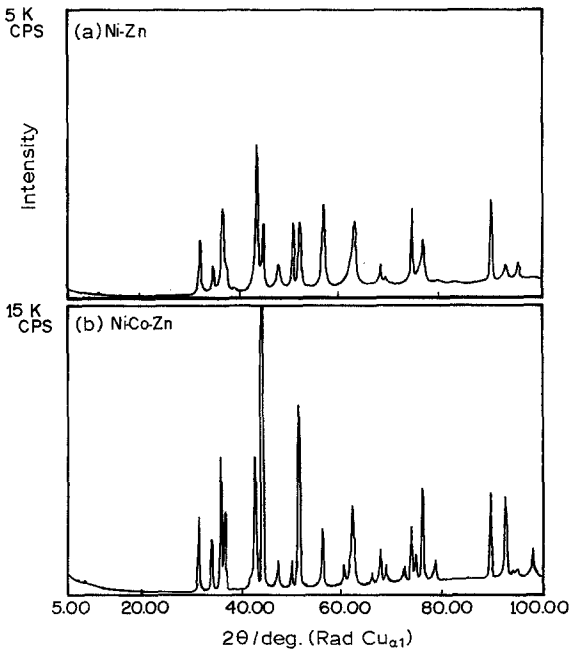

Fig. 2. X-ray diffractograms for (a) Ni–Zn and (b) Ni–Co–Zn after heat treatment in an argon atmosphere at 400°C.

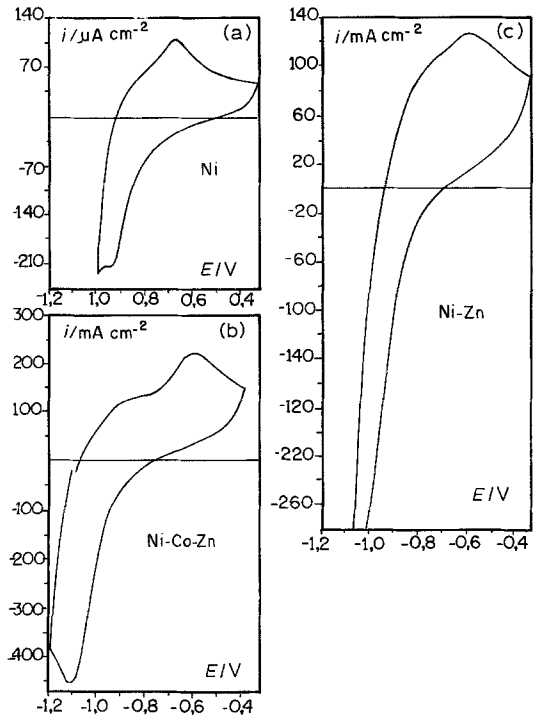

Fig. 3. Steady state cyclic voltammograms for (a) polished Ni, (b) Ni–Co–Zn and (c) Ni–Zn, in 0.5 M NaOH at 25°C. v = 50 mV s^{-1}. Anodic currents taken as positive.

3.2. *Evaluation of the active surface area*

Scanning electron microscopy (SEM) experiments of the surface of the electrodeposits of Ni–Zn and Ni–Co–Zn after leaching, together with that of a polished nickel foil (Carlo ERba 99.5%), show that the surface becomes highly irregular after treatment with KOH, showing a large number of pores. A knowledge of the roughness factor is very important in order to understand the improved behaviour of the material because effects due to an increase in surface area must be separated from those due to real catalytic activity.

In this work the roughness factor was evaluated by cyclic voltammetry. The potential of the electrode was varied in the region -1.20 to -0.35 V against Hg/HgO/0.5 M HO^- where nickel is reversibly oxidated to α–$Ni(OH)_2$. This reaction has been studied by u.v. and visible spectroscopy [17] and it is known to correspond to the formation of a monolayer. This approach is justified by an analysis of published results [6] where the real/apparent areas of coated electrodes calculated from potential decay and BET measurements are similar to those derived from the corresponding cyclic voltammograms. Thus, the size of the anodic peak in the voltammograms was considered to be proportional to the area of the electrode. The voltammograms obtained for polished nickel and for the treated deposits are presented in Fig. 3. The shapes of the curves are somewhat different, reflecting the variations in activity with respect to hydrogen evolution together with the presence of an additional anodic peak probably due to H_{ads} or to hydrides formed in the cathodic sweep. Nevertheless, the peak corresponding to the formation of α–$Ni(OH)_2$ is clearly defined in all cases and was used to evaluate the relative increase in the active area for the deposits, as shown in Table 3.

Table 3. Peak current and increase in area relative to polished nickel from the voltammograms in Fig. 3

	Polished Ni	*Ni–Zn*	*Ni–Co–Zn*
I_p (mA cm^{-2})	0.110	124	220
Relative increase in area	1	1127	2000

3.3 *Catalytic activity for the HER*

Figure 4 shows Tafel plots, corrected for ohmic potential drop and the contribution of the reverse reaction, for Ni–Zn and Ni–Co–Zn in 0.5 M NaOH at 25° C. For comparison, results for bright nickel are included in the same figure. The corresponding electrochemical parameters are presented in Table 4 together with a comparison between the current densities at η = 135 mV which confirms the values of the relative active areas measured by cyclic voltammetry. Table 4 shows that in terms of real area the exchange currents are lower for the deposits than for nickel. However, as discussed by Conway *et al.* [18] the value of the Tafel slope is also very important in determining the activity of a material at a given current density. For this reason, at 135 mA cm^{-2}, the overpotentials of the deposits are significantly lower than for nickel, even after correction for real active area. The behaviour presented by Ni–Zn in Fig. 4 (one slope) does not agree with that reported by Arul Raj and Vasu [15] who observed two slopes for the same material. In particular, they found a much larger Tafel slope in the region of current densities of technological interest (greater than 100 mA cm^{-2}), so their overpotentials are significantly larger than those reported in this work.

Figure 5 shows the Tafel plots for Ni–Zn and Ni–Co–Zn in 28% KOH for different temperatures. The corresponding parameters are presented in Table 5. It is interesting to note that at 135 mA cm^{-2} the overpotentials for the two materials are almost the same at each temperature. This must be due to a compensation between the lower values for i_0 and for b presented by Ni–Zn with respect to Ni–Co–Zn. This also means that at higher current densities Ni–Zn is the better material. An examination of the values in Table 5

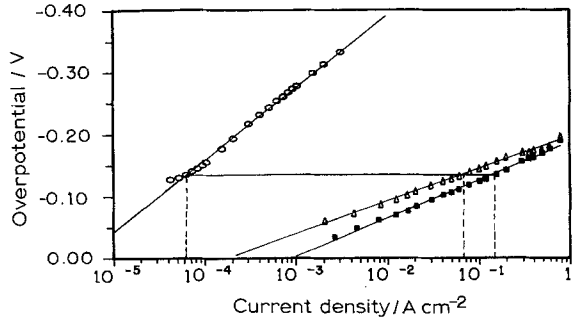

Fig. 4. Tafel plots for (○) polished Ni; (△) Ni–Zn and (■) Ni–Co–Zn in 0.5 M NaOH at 25° C.

Table 4. Tafel parameters from the plots in Fig. 4. b = Tafel slope, $i_{0,g}$ = exchange current density (geometric area), $i_{0,r}$ = exchange current density (real active area). $(i/i_{Ni})_{\eta=135}$ is the current ratio taken from Fig. 4 at η = 135 mV (where i = 135 mA cm^{-2} for Ni–Co–Zn)

Material	$i_{0,g}$/A cm^{-2}	$i_{0,r}$/A cm^{-2}	b/mV dec^{-1}	$(i/i_{Ni})_{\eta=135}$
Polished Ni	3.83×10^{-6}	3.83×10^{-6}	120	1
Ni–Zn	1.89×10^{-4}	1.68×10^{-7}	53	1133
Ni–Co–Zn	8.59×10^{-4}	4.29×10^{-7}	62	2250

indicates that the Tafel slopes do not vary with temperature, contradicting the predictions of the classical theories. This phenomenon has been discussed by Conway *et al.* [19, 20] in terms of the entropic and ethalpic components to the energy of activation, but this has been contested by Gileadi [21] and the conclusion is that at present the problem is not well understood.

The values of the energy of activation for the HER on the two electrode materials, 33 kJ mol^{-1} for Ni–Zn and 24 kJ mol^{-1} for Ni–Co–Zn, were obtained from the corresponding Arrhenius plots (Fig. 6). These were calculated at η = 120 mV to avoid extrapolations. The values are similar to those reported previously for Ni–Mo–Cd (10 and 36 kJ mol^{-1} for low and high c.d., respectively [22]) and somewhat lower than those observed for bright nickel (41 kJ mol^{-1} [22]), porous nickel (42 kJ mol^{-1} [23]) and in the previous study of Ni–Zn (38 kJ mol^{-1} [15]). According to the results in Table 4 the values of the energy of activation should be larger for the deposits than for nickel (provided the mechanism of the reaction is the same). So, at present it is difficult to rationalize the discrepancies. On the other hand, in view of the temperature independence of the Tafel slopes it is not justified to use classical theories to analyse other results.

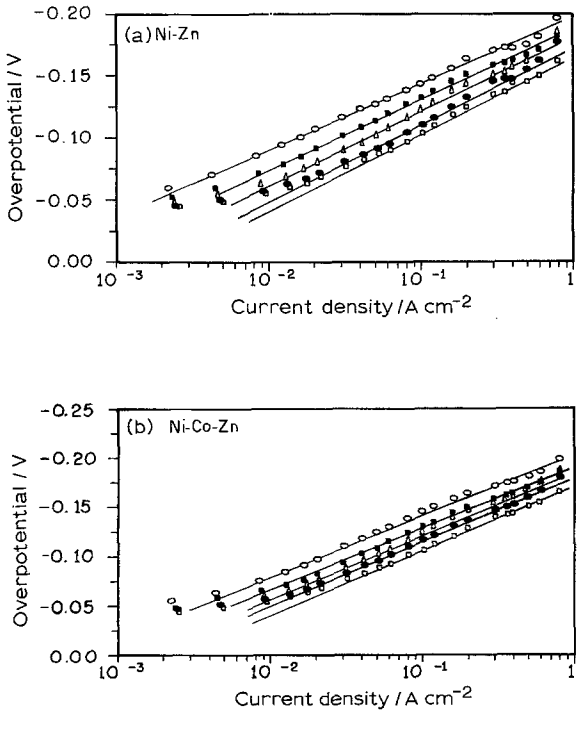

Fig. 5. Tafel plots in 28% KOH and different temperatures for (a) Ni–Zn and (b) Ni–Co–Zn: (○) 25, (■) 40, (△) 50, (●) 60 and (□) 70° C.

Table 5. Electrochemical parameters obtained from the plots in Fig. 5. b = Tafel slope, i_0 = exchange current density, η_{135} = overpotential for a c.d. of 135 mA cm^{-2}

T/°C	Ni–Zn			Ni–Co–Zn		
	b /mV dec^{-1}	$i_0 \times 10^3$ /A cm^{-2}	η_{135} /V	b /mV dec^{-1}	$i_0 \times 10^3$ /A cm^{-2}	η_{135} /V
25	55	0.234	0.152	61	0.475	0.150
40	57	0.499	0.139	64	1.01	0.138
50	60	0.918	0.129	66	1.37	1.132
60	63	1.66	0.119	65	1.59	0.125
70	60	1.82	0.112	62	1.78	0.115

3.4. *Continuous operation*

Continuous operation tests for up to 1800 h were conducted with the 200 cm^2 electrodes in 28% KOH at 70° C under a current density of 135 mA cm^{-2}. The results are shown in Fig. 7. The two electrodeposits give a stable overpotential of about 0.15 V, which is well below the value of 0.38 V measured under the same conditions for mild steel, the traditional material used in unipolar electrolysers. Also, the electrodes showed good mechanical stability and were unaffected by the presence of impurities in the system.

Finally, two systems simulating the operational conditions of actual electrolysers were compared: one with mild steel cathodes and electrodeposited nickel anodes and another with Ni–Co–Zn cathodes and anodes. The results in 28% KOH solutions at 70° C and a current density of 135 mA cm^{-2} show that the codeposits give an operational voltage which is 0.2 V lower. This improved performance is entirely due to the reduced cathodic overvoltage but the experiment also shows that Ni–Co–Zn codeposits are very stable when used as anodes.

Acknowledgements

Thanks are due to the Conselho Nacional de Desenvolvimento Científico e Tecnológico (CNPq) and the Financiadora de Estudos e Projetos (FINEP) for financial support.

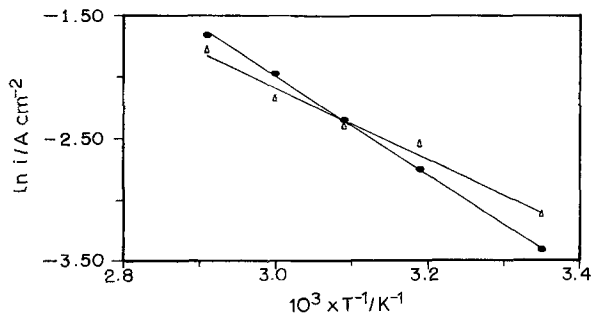

Fig. 6. Arrhenius plots for (●) Ni–Zn and (△) Ni–Co–Zn.

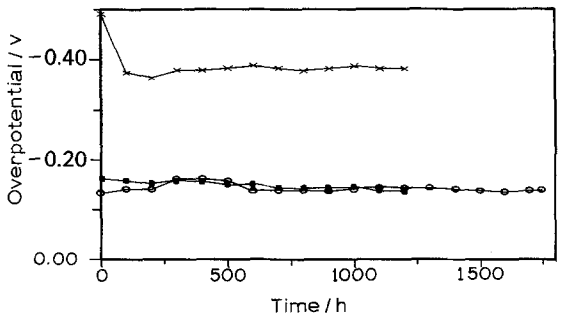

Fig. 7. Potential–time characteristics for (×) mild steel; (■) Ni–Zn; (○) Ni–Co–Zn 200 cm^2 electrodes in 28% KOH at 70° C under a c.d. of 135 mA cm^{-2}.

References

[1] R. L. Le Roy. *Int. J. Hydrogen Energy* **8** (1983) 1.

[2] B. V. Tilak and S. Srinivasan, *in* 'Handbook of energy systems engineering' (edited by B. V. Tilak, S. Srinivasan, T. C. Varijen and R. J. Pryputniewicz), J. Wiley & Sons, New York (1985).

[3] J. O'M. Bockris, *in* 'Comprehensive treatise of electrochemistry' (edited by J. O'M Bockris, E. Yeager, B. E. Conway and R. White), Vol. 3, Plenum Press, New York (1985).

[4] H. Wendt and G. Imarisio, *J. Appl. Electrochem.* **18** (1988) 1.

[5] B. E. Conway, L. Bai and D. F. Tessier, *J. Electroanal. Chem.* **161** (1984) 39.

[6] B. E. Conway and L. Bai, *J. Chem. Soc., Faraday Trans. 1* **81** (1985) 1841.

[7] H. Vanderborre, Ph. Vermeiren and R. Leysen, *Electrochim. Acta* **29** (1984) 297.

[8] R. Sabela and I. Paseka, *J. Appl. Electrochem.* **20** (1990) 500.

[9] E. Endoh, H. Otouma, T. Morimoto and Y. Oda, *Int. J. Hydrogen Energy* **12** (1987) 473.

[10] Y. Choquette, L. Brossard and H. Ménard, (a) *J. Appl. Electrochem.* **20** (1990) 855; (b) *Int. J. Hydrogen Energy* **15** (1990) 551.

[11] G. Fiori and C. M. Mari, *Int. J. Hydrogen Energy* **12** (1987) 159.

[12] E. R. Gonzalez, L. A. Avaca, A. Carubelli, A. A. Tanaka and G. Tremiliosi-Filho, *ibid* **9** (1984) 689.

[13] J. de Carvalho, G. Tremiliosi-Filho, L. A. Avaca and E. R. Gonzalez, *ibid.* **14** (1989) 161.

[14] (a) J. Divisek, P. Malinowski, J. Mergel and H. Schmitz, *Int. J. Hydrogen Energy* **13** (1988) 141; (b) J. Divisek, H. Schmitz and J. Balej, *J. Appl. Electrochem.* **19** (1989) 519.

[15] I. Arul Raj and K. I. Vasu, *J. Appl. Electrochem.* **20** (1990) 32.

[16] B. V. Tilak, A. C. Ramamurthy and B. E. Conway, *Proc. Indian Acad. Sci. (Chem. Sci.)* **97** (1986) 359.

[17] F. Hahn, B. Beden, M. J. Croissant and C. Lamy, *Electrochim. Acta.* **31** (1986) 35.

[18] B. E. Conway, L. Bai and M. A. Sattar, *Int. J. Hydrogen Energy* **12** (1987) 607.

[19] B. E. Conway, D. F. Tessier and D. P. Wilkinson, *J. Electroanal. Chem.* **199** (1986) 249.

[20] *Idem, J. Electrochem. Soc.* **136** (1989) 2486.

[21] E. Gileadi, *J. Electrochem. Soc.* **134** (1987) 117.

[22] B. E. Conway and L. Bai, *Int. J. Hydrogen Energy* **111** (1986) 533.

[23] H. Wendt and V. Plzak, *Electrochim. Acta* **28** (1983) 27.